



The Deformation of Steep Surface Waves on Water. I. A Numerical Method of Computation

M. S. Longuet-Higgins; E. D. Cokelet

Proceedings of the Royal Society of London. Series A, Mathematical and Physical Sciences, Vol. 350, No. 1660. (Jul. 30, 1976), pp. 1-26.

Stable URL:

<http://links.jstor.org/sici?sici=0080-4630%2819760730%29350%3A1660%3C1%3ATDOSSW%3E2.0.CO%3B2-H>

Proceedings of the Royal Society of London. Series A, Mathematical and Physical Sciences is currently published by The Royal Society.

Your use of the JSTOR archive indicates your acceptance of JSTOR's Terms and Conditions of Use, available at <http://www.jstor.org/about/terms.html>. JSTOR's Terms and Conditions of Use provides, in part, that unless you have obtained prior permission, you may not download an entire issue of a journal or multiple copies of articles, and you may use content in the JSTOR archive only for your personal, non-commercial use.

Please contact the publisher regarding any further use of this work. Publisher contact information may be obtained at <http://www.jstor.org/journals/rsl.html>.

Each copy of any part of a JSTOR transmission must contain the same copyright notice that appears on the screen or printed page of such transmission.

The JSTOR Archive is a trusted digital repository providing for long-term preservation and access to leading academic journals and scholarly literature from around the world. The Archive is supported by libraries, scholarly societies, publishers, and foundations. It is an initiative of JSTOR, a not-for-profit organization with a mission to help the scholarly community take advantage of advances in technology. For more information regarding JSTOR, please contact support@jstor.org.

The deformation of steep surface waves on water

I. A numerical method of computation

BY M. S. LONGUET-HIGGINS, F.R.S. AND E. D. COKELET

Department of Applied Mathematics and Theoretical Physics,

University of Cambridge, England, and

Institute of Oceanographic Sciences, Wormley, Godalming, Surrey

(Received 28 October 1975)

Plunging breakers are beyond the reach of all known analytical approximations. Previous numerical computations have succeeded only in integrating the equations of motion up to the instant when the surface becomes vertical. In this paper we present a new method for following the time-history of space-periodic irrotational surface waves. The only independent variables are the coordinates and velocity potential of marked particles at the free surface. At each time-step an integral equation is solved for the new normal component of velocity. The method is faster and more accurate than previous methods based on a two dimensional grid. It has also the advantage that the marked particles become concentrated near regions of sharp curvature. Viscosity and surface tension are both neglected.

The method is tested on a free, steady wave of finite amplitude, and is found to give excellent agreement with independent calculations based on Stokes's series. It is then applied to unsteady waves, produced by initially applying an asymmetric distribution of pressure to a symmetric, progressive wave. The freely running wave then steepens and overturns. It is demonstrated that the surface remains rounded till well after the overturning takes place.

1. INTRODUCTION

Breaking waves are the agent for many significant processes in the upper ocean including the transfer of horizontal momentum from wind-waves to surface currents. Yet remarkably, one of the most familiar and spectacular properties of the sea surface—its capacity to turn over on itself—is one of the least well understood. All the usual theories for surface waves—the small-amplitude approximations of Airy and Stokes, the nonlinear shallow-water theory and the Korteweg–De Vries equations for solitary and cnoidal waves—are essentially approximations, valid only when the fluid acceleration is sufficiently small compared to gravity. These approximate theories cease to be valid when the acceleration is comparable to g , or when the surface elevation is a multivalued function of the horizontal displacement.

The small-amplitude theories can indeed be carried to higher approximations, showing that the form of steady waves of large amplitude tends, in the limit, to the simple corner-flow discovered by Stokes (1880*a*) in which the free surface has a sharp

angle of 120° . But these theories are for steady, symmetric waves, and do not describe the development of the flow as the surface overturns. An attempt was made by Price (1971) to construct a perturbation of Stokes's corner-flow, but his expressions contain singularities for both $t > 0$ and $t < 0$ (both after *and* before the break point) and so do not represent an appropriate solution.

An oft-quoted theory for wave breaking is that of Biesel (1952) who carried to a second approximation Miche's first-order Lagrangian solution for waves approaching a plane beach. In this theory, the free surface appears to develop a cusp, and then intersects itself, forming a closed loop. It hardly needs to be pointed out that the approximation ceases to be valid long before the cusp is formed, and moreover that the looped surface is topologically impossible, if the fluid is to lie always on one side of the free surface.

The mathematical difficulty of the problem arises essentially from the need to satisfy the condition of constant pressure (which is generally non-linear in the velocity) at a free surface which not only is unknown, but whose form is highly time-dependent. Since no appropriate analytical theory has yet been suggested, it is natural to seek whatever guidance can be got from numerical computations. A start in this direction was made by Chan & Street (1970), who employed the so-called 'marker-and-cell' technique. The flow being assumed two dimensional (that is, dependent only on the coordinates x, y and on the time t), the (x, y) -plane is covered by a rectangular grid, and the velocity components are computed at fixed points within each cell. The development of the flow is followed in small time-steps, using difference-equations to represent the conservation of mass and momentum (the fluid being assumed incompressible and inviscid). For waves in water of finite uniform depth, this method achieved some success. The authors were able to demonstrate, for example, the steepening of the forward face of the wave almost up to the instant when the free surface becomes vertical. A description of the overturning was not achieved, though the computational procedure might, with further trouble, have been modified so as to cope with a multivalued surface elevation. It is notable that in these computations no use was made of the vorticity equation; it was assumed simply that the *initial* flow was irrotational. At subsequent times the flow was not quite irrotational.

Now all numerical computations using a rectangular grid have an important practical limitation. To obtain acceptable accuracy, the grid-spacing must be reasonably small, at least compared to the local scale of the flow or the radius of curvature of the free surface. But as the spacing is reduced, the number of grid points has to increase like N^2 , where N is the order of magnitude of the number of points in each direction. In this way, the quick-access storage of even the larger computers is rapidly used up, and the necessary computation time also exceeds practical limitations.

To overcome these essential difficulties we have developed and tested a quite different numerical method, which we describe in the present paper.

For oscillatory waves, the diffusion of vorticity into the interior may be quite slow

(see Longuet-Higgins 1953*b*, 1960). Hence, up to the point of breaking it may be a good approximation to neglect viscosity and assume the motion irrotational. This leads to a velocity potential satisfying Laplace's equation ($\nabla^2\phi = 0$). Now within a closed boundary such functions are uniquely determined by their values on the boundary itself. Moreover the time-evolution of the flow is uniquely determined by the pressure applied at the moving surface, through Bernoulli's equation. Hence the problem is in reality a problem in one space dimension, not two.

Using this insight, and assuming the motion to be periodic in space (though not necessarily in time) we first transform the coordinates so that the domain of the fluid lies within a simple closed contour. The boundary C corresponds to the free surface. We then show that for particles on the surface, the kinematical and dynamical conditions can be very simply expressed in terms of the rates of change of ϕ and of the coordinates *following a fixed particle*. It follows that by proceeding in small time-steps we are able to follow the potential ϕ from one position of the free surface to the succeeding position. This does not alone solve the problem, however. From the values of ϕ on the new position of the surface we can indeed calculate the tangential component of velocity $\partial\phi/\partial s$. But for the next step we need also to know the normal component $\partial\phi/\partial n$. The crucial step is to determine $\partial\phi/\partial n$ at each point of the boundary by the solution of an integral equation (equation (4.5) below). Once this is done, with sufficient accuracy, the time-stepping can proceed.

It will be apparent that this mixed Eulerian-Lagrangian method has the outstanding advantage that the independent variables are all evaluated at the free surface. The velocity potential and its derivatives in the interior are not used, though these can easily be calculated from surface values by Cauchy's theorem. Hence the number of independent variables in the computation is of order N , not N^2 , and for given storage and machine-time much greater accuracy can be obtained.

The method is also flexible. Not only free waves can be computed, but also waves to which is applied any smooth distribution of pressure at the free surface.

One welcome but unexpected advantage is also the tendency of the marked particles to concentrate near regions of sharp curvature, where accurate resolution is most needed.

The accurate programming of the computation is an essential and by no means trivial task, described below in §§ 5–8. As will be seen, one of the keys to success was to devise a simple smoothing technique, which eliminated certain unwanted instabilities.

The method was first tested on the special case of a free progressive wave of finite amplitude, for which accurate and independent methods of computation have recently become available. As will be seen from § 9, the present time-stepping technique was in excellent agreement with the independent computation. Then as a first application of the method, we describe in § 10 the development of a free wave which by an initial application of surface pressure is raised to an energy level exceeding the maximum for a steady, progressive wave. Figures 6–12 show how the

wave develops in time, ultimately turning over and plunging towards the forward face of the wave.

Some of the implications of this straightforward calculation are discussed in § 11. This paper is intended to be the first of a series in which the present method of computation is employed as one tool in a systematic investigation of free surface flows and breaking waves.

2. BASIC EQUATIONS

Let (x, y) denote rectangular coordinates with the x -axis horizontal and the y -axis vertical, as in figure 1. The motion is assumed to be periodic in the x -direction, with period

$$L = 2\pi/k. \quad (2.1)$$

The fluid is inviscid and incompressible, and the origin is taken to be in the mean surface level. The motion may be assumed to be started from rest by conservative forces, so that it is irrotational at all times; any slow diffusion of vorticity inwards

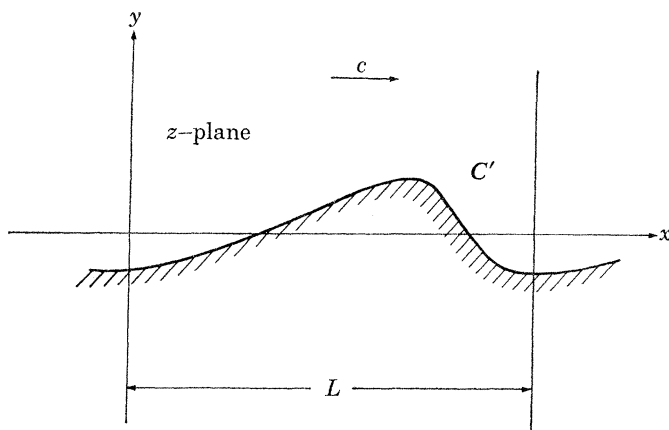


FIGURE 1. Choice of axes and notation for space-periodic wave motion in deep water.

from the boundaries is neglected. By a choice of reference frame, the x -averaged horizontal velocity \bar{u} at some given depth y may be taken as zero and then, since the motion is periodic and irrotational, \bar{u} must vanish at all other depths y (beneath the lowest point of the free surface). Thus

$$\bar{u} = 0 \quad (2.2)$$

at all depths, and also at all times, since a non-zero value of $\partial\bar{u}/\partial t$ would imply an infinite rate of input of horizontal momentum.

It is convenient to choose units of mass, length and time so that the density ρ is unity and also so that

$$g = 1, \quad k = 1, \quad (2.3)$$

where g is the acceleration due to gravity. By (2.1) we have then

$$L = 2\pi. \quad (2.4)$$

We have now the following equations for the velocity potential ϕ . Since the fluid is irrotational and incompressible

$$\mathbf{u} = \nabla\phi, \quad \nabla \cdot \mathbf{u} = \nabla^2\phi = 0. \quad (2.5)$$

Since $\nabla\phi$ is periodic and $\overline{\nabla\phi} = 0$, it may be shown (Longuet-Higgins 1953*a*) that at great depths $\nabla\phi$ vanishes exponentially:

$$|\nabla\phi| \leq A(x, t)e^{\nu}. \quad (2.6)$$

At the free surface $y = y_s(x, t)$ we have the kinematic conditions

$$\frac{Dx}{Dt} = \frac{\partial\phi}{\partial x}, \quad \frac{Dy}{Dt} = \frac{\partial\phi}{\partial y}, \quad (2.7)$$

where

$$\frac{D}{Dt} = \frac{\partial}{\partial t} + \nabla\phi \cdot \nabla, \quad (2.8)$$

which denotes differentiation following a given particle. We have also the dynamical condition derived from Bernoulli's equation, namely that

$$\partial\phi/\partial t = -p_s - y - \frac{1}{2}(\nabla\phi)^2, \quad (2.9)$$

where p_s denotes the pressure applied at the surface. From this we can immediately derive the rate of change of ϕ following the motion, namely

$$D\phi/Dt = -p_s - y + \frac{1}{2}(\nabla\phi)^2. \quad (2.10)$$

The difference between the right-hand sides of (2.9) and (2.10) is simply a change of sign in the last term.

3. TRANSFORMATION OF COORDINATES

Since the motion is periodic in x with period 2π we may write

$$r e^{i\theta} = \zeta = e^{-iz} \quad (z = x + iy), \quad (3.1)$$

where ζ is a new complex variable, analytic and single-valued everywhere inside the contour C which corresponds to the fluid surface (see figure 2). (r, θ) are polar coordinates in the ζ -plane, and we have from (3.1)

$$\left. \begin{aligned} r &= e^{\nu}, & y &= \ln r, \\ \theta &= -x, & x &= -\theta. \end{aligned} \right\} \quad (3.2)$$

All points at infinite depth in the (x, y) plane are transformed into the origin O in the ζ -plane.

Let us write

$$\chi = \phi + i\psi \quad (3.3)$$

for the complex velocity-potential in the physical (x, y) -plane. Then χ is generally analytic and single-valued inside C . Moreover by equation (2.6) it follows that as $\zeta \rightarrow 0$

$$\chi \sim A\zeta. \quad (3.4)$$

Hence χ is analytic and single-valued everywhere inside C .

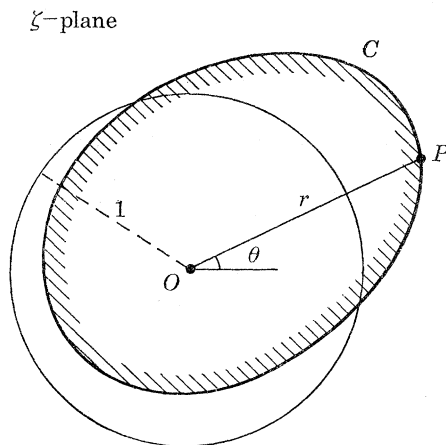


FIGURE 2. One wavelength in the z -plane transformed to a closed domain in the ζ -plane by equation (3.1). The free surface is transformed into the contour C .

At the free surface we have from (2.7) and (3.2)

$$\left. \begin{aligned} \frac{Dr}{Dt} &= e^y \frac{Dy}{Dt} = r \frac{\partial \phi}{\partial y} = r^2 \frac{\partial \phi}{\partial r}, \\ \frac{D\theta}{Dt} &= -\frac{Dx}{Dt} = -\frac{\partial \phi}{\partial x} = \frac{\partial \phi}{\partial \theta}. \end{aligned} \right\} \quad (3.5)$$

Lastly, since

$$\left(\frac{\partial \phi}{\partial x} \right)^2 + \left(\frac{\partial \phi}{\partial y} \right)^2 = \left| \frac{d\chi}{dz} \right|^2 = \left| \frac{d\zeta}{dz} \right|^2 \left| \frac{d\chi}{d\zeta} \right|^2 = r^2 \left[\left(\frac{\partial \phi}{\partial r} \right)^2 + \left(\frac{1}{r} \frac{\partial \phi}{\partial \theta} \right)^2 \right]$$

the dynamical condition (2.10) becomes

$$\frac{D\phi}{Dt} = -p_s - \ln r + \frac{1}{2} \left[\left(r \frac{\partial \phi}{\partial r} \right)^2 + \left(\frac{\partial \phi}{\partial \theta} \right)^2 \right]. \quad (3.6)$$

4. THE DIRICHLET PROBLEM

Suppose that at some initial instant $t = t_0$ we are given the velocity potential ϕ throughout the fluid, and hence the value of ϕ and its derivatives both inside and on the contour $C(t_0)$. Let (r, θ) denote the (Lagrangian) coordinates of a particle on

$C(t_0)$. Then equations (3.5) will determine the position of the same particle a short time dt later. Similarly (3.6) will determine the value of $\phi(t_0 + dt)$ on the new contour $C(t_0 + dt)$. By considering adjacent particles, and differentiating along the surface we can then obtain the *tangential* component of velocity $\partial\phi/\partial s$. But this does not immediately determine the normal component $\partial\phi/\partial n$, which is also needed for the step afterwards.

The problem of determining the normal component of velocity at the boundary is equivalent to the *Dirichlet problem* of finding the normal gradient of a function ϕ

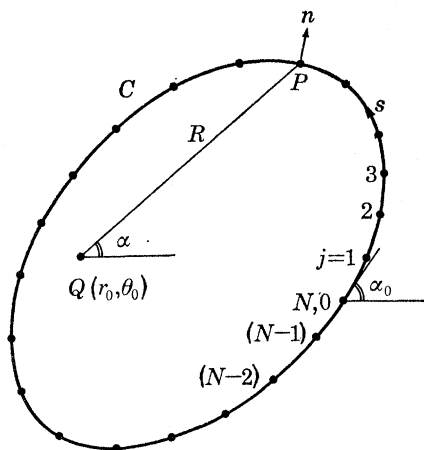


FIGURE 3. Definition of variables for the Dirichlet problem of § 4.

whose values are given on a closed contour C , and which is harmonic ($\nabla^2\phi = 0$) everywhere inside C . We may formulate the problem as an integral equation as follows.

Let (s, n) be tangential and normal coordinates at a typical point P on the boundary (see figure 3), and let (R, α) be the polar coordinates of P with respect to an arbitrary point $Q(r_0, \theta_0)$ in the interior. Let

$$S = \frac{1}{2\pi} \ln R \tag{4.1}$$

so $\nabla^2 S = 0$. Then by Green's theorem we have

$$\begin{aligned} \phi(r_0, \theta_0) &= \int_C \left(\phi \frac{\partial S}{\partial n} - \frac{\partial \phi}{\partial n} S \right) ds \\ &= \frac{1}{2\pi} \int_C \left(\phi \frac{\partial \alpha}{\partial s} - \frac{\partial \phi}{\partial n} \ln R \right) ds. \end{aligned} \tag{4.2}$$

Denoting $\phi(r_0, \theta_0)$ by ϕ_0 , we have then

$$2\pi\phi_0 = \int_C \phi d\alpha - \int_C \frac{\partial \phi}{\partial n} \ln R ds. \tag{4.3}$$

Letting $Q(r_0, \theta_0)$ approach C , we have in the limit

$$\int_C \phi \, d\alpha = \pi\phi_0 + P \int_C \phi \, d\alpha, \quad (4.4)$$

where P denotes the principal value (C is assumed to be a smooth at Q). Hence altogether from (4.3) and (4.4)

$$\int_C \frac{\partial\phi}{\partial n} \ln R \, ds = P \int_C \phi \, d\alpha - \pi\phi_0. \quad (4.5)$$

Since the right-hand side involves only the values of ϕ on C , which are known, and since R, α are determined solely by the shape of C , equation (4.5) is an integral equation for $(\partial\phi/\partial n)$, with a singular kernel $\ln R$.

It remains to express the time-derivatives of r, θ and ϕ in terms of the tangential and normal derivatives of ϕ . We have in general

$$\frac{\partial}{\partial r} = \cos\beta \frac{\partial}{\partial s} + \sin\beta \frac{\partial}{\partial n},$$

$$\frac{1}{r} \frac{\partial}{\partial \theta} = \sin\beta \frac{\partial}{\partial s} - \cos\beta \frac{\partial}{\partial n},$$

where $\cos\beta = \frac{\partial r}{\partial s}, \quad \sin\beta = r \frac{\partial \theta}{\partial s}.$

Hence equations (3.5) and (3.6) become

$$\left. \begin{aligned} \frac{Dr}{Dt} &= r^2 \frac{\partial r}{\partial s} \frac{\partial \phi}{\partial s} + r^3 \frac{\partial \theta}{\partial s} \frac{\partial \phi}{\partial n}, \\ \frac{D\theta}{Dt} &= r^2 \frac{\partial \theta}{\partial s} \frac{\partial \phi}{\partial s} - r \frac{\partial r}{\partial s} \frac{\partial \phi}{\partial n}, \\ \frac{D\phi}{Dt} &= -p_s - \ln r + \frac{1}{2} r^2 \left[\left(\frac{\partial \phi}{\partial s} \right)^2 + \left(\frac{\partial \phi}{\partial n} \right)^2 \right]. \end{aligned} \right\} \quad (4.6)$$

Equations (4.5) and (4.6), together with initial conditions, are the basis for the following computations.

5. SOLUTION OF THE INTEGRAL EQUATION

The values of $\phi, \partial\phi/\partial s$ and $\partial\phi/\partial n$ are to be evaluated at a finite number N of points on the boundary which will correspond to fixed particles. We label these with the suffix j , where $j = 1, 2, \dots, N$. The corresponding values of r, θ are similarly labelled r_j, θ_j . We will suppose that Q lies in turn at (r_i, θ_i) where $i = 1, 2, \dots, N$ also. Hence R, α, s take the values $R_{ij}, \alpha_{ij}, s_{ij}$. The integral on the left of (4.5) can be approximated as the product of the $(N \times 1)$ matrix $(\partial\phi/\partial n)_j$ multiplied by an $(N \times N)$ matrix

of coefficients, say A_{ij} . The integral on the right can be approximated by a quantity B_i . Hence we have N linear simultaneous equations of the form

$$A_{ij}(\partial\phi/\partial n)_j = B_i \quad (i = 1, \dots, N) \quad (5.1)$$

to be solved for the values $(\partial\phi/\partial n)_j$.

The success of the method will depend critically upon the accuracy with which the integrals in equation (4.5) are approximated by linear sums. Let i be fixed, and let us take $Q(r_i, \theta_i)$ as origin of s , writing $s_{ij} = s_{(j-i) \bmod N}$. Since $\ln R$ is singular both at $s = 0$ and $s = s_N$, but $\ln(R/s)$ or $\ln[R/(s_N - s)]$ is not, we write the integral on the left of (4.5) as follows

$$\int_C \frac{\partial\phi}{\partial n} \ln R \, ds = \int_0^{s_L} \frac{\partial\phi}{\partial n} \ln(R/s) \, ds + \int_0^{s_L} \frac{\partial\phi}{\partial n} \ln s \, ds + \int_{s_L}^{s_M} \frac{\partial\phi}{\partial n} \ln R \, ds \\ + \int_{s_M}^{s_N} \frac{\partial\phi}{\partial n} \ln\left(\frac{R}{s_N - s}\right) \, ds + \int_{s_M}^{s_N} \frac{\partial\phi}{\partial n} \ln(s_N - s) \, ds, \quad (5.2)$$

where s_L is the arclength at a point close to $s = 0$ and on the positive side, and s_M is a similar arclength just short of the other end of the range of integration. (In our calculation we take s_L to be the larger of s_6 and $0.1s_N$ and s_M to be the smaller of s_{N-5} and $0.9s_N$.)

We denote the integrals in (5.2) by I_1, I_2, \dots, I_5 respectively. I_1, I_3 and I_4 are no longer singular, and may be calculated by approximating the integrand over each sub-interval (s_j, s_{j+1}) by a 4-point Lagrangian polynomial. More specifically, a 4-point, closed-range quadrature formula is used at the end-points of each integral, and a 4-point, open-range quadrature formula is used for the remainder (Buckingham, 1962). The local errors in this method are of order $(\Delta s)^5$, where Δs is the maximum arclength between two adjacent points s_j .

The remaining integrals I_2 and I_5 must be handled differently. I_2 for example, can be written as the sum of integrals of the form

$$\int_{s_j}^{s_{j+1}} \frac{\partial\phi}{\partial n} \ln s \, ds = \int_{s_j}^{s_{j+1}} \left[\left(\frac{\partial\phi}{\partial n}\right)_j + (s - s_j) \left(\frac{\partial}{\partial s} \frac{\partial\phi}{\partial n}\right)_j + \dots + \frac{(s - s_j)^4}{4!} \left(\frac{\partial^4}{\partial s^4} \frac{\partial\phi}{\partial n}\right)_j + \dots \right] \ln s \, ds. \quad (5.3)$$

Each term in the integrand can be evaluated exactly. To find the derivatives of $\partial\phi/\partial n$ with respect to s , we approximated $(\partial\phi/\partial n)_j$ by a fourth-order Lagrangian interpolation polynomial over the 5 points centred on j , and differentiated this. The integral I_5 is handled in a similar way, except centred on the point $(j + 1)$. This technique gives local errors of order $(\Delta s)^6 \ln(\Delta s)$.

To calculate the arclengths s_j , the quantities r_j and $(\theta_j - 2\pi j/N)$ as functions of j (considered as a real variable) were approximated by cubic splines (see Ahlberg, Nilson & Walsh 1967). From these can be calculated dr/dj , $d\theta/dj$ and hence

$$\frac{ds}{dj} = \left[\left(\frac{dr}{dj}\right)^2 + \left(r \frac{d\theta}{dj}\right)^2 \right]^{\frac{1}{2}} \quad (5.4)$$

at each point j . Equation (5.4) was then integrated by Simpson's rule, giving s_j at

each point, with local errors of order $(\Delta s)^4$. The tangential derivative $d\phi/dj$ was calculated similarly. Hence we found

$$\left. \begin{aligned} \left(\frac{\partial r}{\partial s}\right)_j &= \left(\frac{dr}{dj}\right)_j / \left(\frac{ds}{dj}\right)_j, \\ \left(\frac{\partial \theta}{\partial s}\right)_j &= \left(\frac{d\theta}{dj}\right)_j / \left(\frac{ds}{dj}\right)_j, \\ \left(\frac{\partial \phi}{\partial s}\right)_j &= \left(\frac{d\phi}{dj}\right)_j / \left(\frac{ds}{dj}\right)_j, \end{aligned} \right\} \quad (5.5)$$

with errors of order $(\Delta s)^3$.

To evaluate the integral on the right-hand side of (4.5) we need to know α_j at each point of the contour. In general we have

$$\alpha_j = \alpha_{j,i} = \arctan \left(\frac{r_j \sin \theta_j - r_i \sin \theta_i}{r_j \cos \theta_j - r_i \cos \theta_i} \right) \quad (j \neq i) \quad (5.6)$$

and in the exceptional case we may use

$$\alpha_i = \alpha_{i,i} = \arctan \left(\frac{\sin \theta_i (dr/dj)_i + r \cos \theta (d\theta/dj)_i}{\cos \theta_i (dr/dj)_i - r \sin \theta (d\theta/dj)_i} \right). \quad (5.7)$$

Because the curve is a simple closed contour we have $\alpha_N = \alpha_i + \pi$. The right hand side of (4.5) can now be written

$$P \int_C \alpha \frac{\partial \phi}{\partial s} ds = P \int_C \alpha \frac{d\phi}{dj} dj \quad (5.8)$$

and integrated using Simpson's rule, since we know the integrand at equally spaced values of j . This gives local errors of order $(\Delta s)^4$.

The above method of solving the integral equation was programmed in FORTRAN IV and solved on the I.B.M. 370/165 digital computer at Cambridge University. With $N = 60$ points along the free surface, the central processing time was 3.4 s and the core-store 150 K bytes for a double-precision calculation (17 significant figures). About 80 % of this time was used to set up the 60×60 system of linear equations, and 20 % was used to invert the matrix. The errors in $\partial\phi/\partial n$ were found to decrease like $(\Delta s)^3$, which is consistent with the errors in the least-accurately determined integral. The computation time varied roughly as N^2 .

6. TIME-STEPPING

For numerical purposes, equations (4.6) may be regarded as first-order ordinary differential equations in t . For most of the time-stepping we used the Adams-Bashforth-Moulton (A.B.M.) scheme which, applied to an equation of the form

$$dy/dt = f(t) \quad (6.1)$$

is as follows:

$$\left. \begin{aligned} y_{1p} &= y_0 + \frac{\Delta t}{24} (55f_0 - 59f_{-1} + 37f_{-2} - 9f_{-3}), \\ y_{1c} &= y_0 + \frac{\Delta t}{24} (9f_{1p} + 19f_0 - 5f_{-1} + f_{-2}). \end{aligned} \right\} \quad (6.2)$$

Here Δt denotes the short time interval, f_n denotes $f(t + n\Delta t)$ and y_{1p} , y_{1c} denote the 'predicted' and 'corrected' values of y_1 (see Acton 1970). The method is fourth-order, local errors being $O(\Delta t)^5$, but requires only two evaluations of f at each time step. Applied to equations (4.6) this means that we have to solve the integral equation for $\partial\phi/\partial n$ only twice for each time-step.

Since the A.B.M. method needs information from three previous time-steps, a fourth order Runge-Kutta (R.K.) technique was used to make the first three time-steps from the initial conditions (see Gerald 1970). This method uses no information about previous time-steps, but takes four mini-steps forward from the current time. A weighted average is then used to calculate the function at the new time. The R.K. method requires four evaluations of the time-derivative at each step and is thus twice as time-consuming as A.B.M.

7. CHECKS OF ACCURACY

The accuracy of our numerical solution to the integral equation (4.5) was tested by calculating, at each time-step, the value of

$$\Omega = \int_C \frac{\partial\phi}{\partial n} ds. \quad (7.1)$$

This represents the total 'outflow' across C in the ζ -plane, or across C' in the z -plane, and it is clear from Green's theorem, or from considerations of continuity, that Ω should vanish identically. The numerical value of Ω was found by writing

$$\Omega = \int_C \frac{\partial\phi}{\partial n} \frac{ds}{dj} dj \quad (7.2)$$

and integrating by Simpson's rule.

As further checks we calculated in a similar way the mean level

$$\bar{y}_s = \frac{1}{2\pi} \int_0^{2\pi} y_s dx = -\frac{1}{2\pi} \int_0^{2\pi} \ln r d\theta \quad (7.3)$$

which also should vanish, and the potential and kinetic energies

$$V = \frac{1}{2\pi} \int_0^{2\pi} \frac{1}{2} y_s^2 dx = \frac{1}{4\pi} \int_0^{2\pi} (\ln r)^2 d\theta \quad (7.4)$$

and

$$T = \frac{1}{2\pi} \int_0^{2\pi} \int_{-\infty}^{y_s} \frac{1}{2} (\nabla\phi)^2 dx dy = \frac{1}{4\pi} \int_C \phi \frac{\partial\phi}{\partial n} \partial s \quad (7.5)$$

(the last step follows from Green's theorem). When there is no input of energy by normal pressure at the surface, then $E = (T + V)$ should remain constant.

All these tests verified the accuracy of our solutions, generally to an acceptable number of decimal places (see below, §§ 9 and 10).

The maximum allowable step Δt should ideally be determined by considerations of accuracy and stability. There being no theory directly applicable to the system (4.6) we have adopted a practical criterion similar to that of Chan & Street (1970) (though their method of dividing the fluid region into cells is quite different from ours). Thus Δt is restricted so that at each step no fluid particle moves more than a distance $(\Delta s)_{\min}$, the minimum arclength from a particle to its nearest neighbour on C . If during the calculation this limit is exceeded, then Δt is halved, and the time-stepping is restarted with three R.K. steps followed by A.B.M. steps as before.

8. INSTABILITY AND SMOOTHING

In nearly all computations, the wave profile, after a sufficiently long time, developed a saw-toothed appearance, in which the computed positions of the particles lay alternately above and below a smooth curve (see, for example, figure 4). The cause of the instability is unknown. Tests showed that, once started, the rate of growth of the instability, per unit time, was independent of the number of time-steps. Hence it is not due simply to rounding errors. The growth may be partly physical, being similar to the growth of short gravity-waves by horizontal compression of the crests of longer waves (see Longuet-Higgins & Stewart 1960; Phillips & Banner 1974). In reality these instabilities are partly damped by viscosity, which we have neglected.

The instability was effectively removed by the following procedure. A function $f(x)$ defined at equally spaced points x_j ($j = 1, 2, 3, \dots$), and in which *alternate* points lie on a smooth curve, can be locally approximated by two polynomials, say

$$h(x) = (a_0 + a_1x + a_2x^2 + \dots + a_nx^n) + (-1)^j (b_0 + b_1x + \dots + b_{n-1}x^{n-1}). \quad (8.1)$$

The first bracket represents a smooth mean curve, the remainder a quantity which oscillates with period 2 in j . The coefficients a_0, a_1, \dots and b_0, b_1, \dots may be chosen uniquely so that $h(x) = f(x)$ exactly at $(2n+1)$ consecutive points x_j , say $(j-n)$ to $(j+n)$ inclusive. As a *smoothed* function we can then take the *even* part:

$$\overline{h(x)} = a_0 + a_1x + a_2x^2 + \dots + a_nx^n. \quad (8.2)$$

In the case $n = 2$ this leads to the 5-point smoothing formula

$$\overline{f_j} = \frac{1}{16}(-f_{j-2} + 4f_{j-1} + 10f_j + 4f_{j+1} - f_{j+2}) \quad (8.3)$$

and when $n = 3$ we find in a similar way

$$\overline{f_j} = \frac{1}{32}(-f_{j-3} + 9f_{j-1} + 16f_j + 9f_{j+1} - f_{j+3}). \quad (8.4)$$

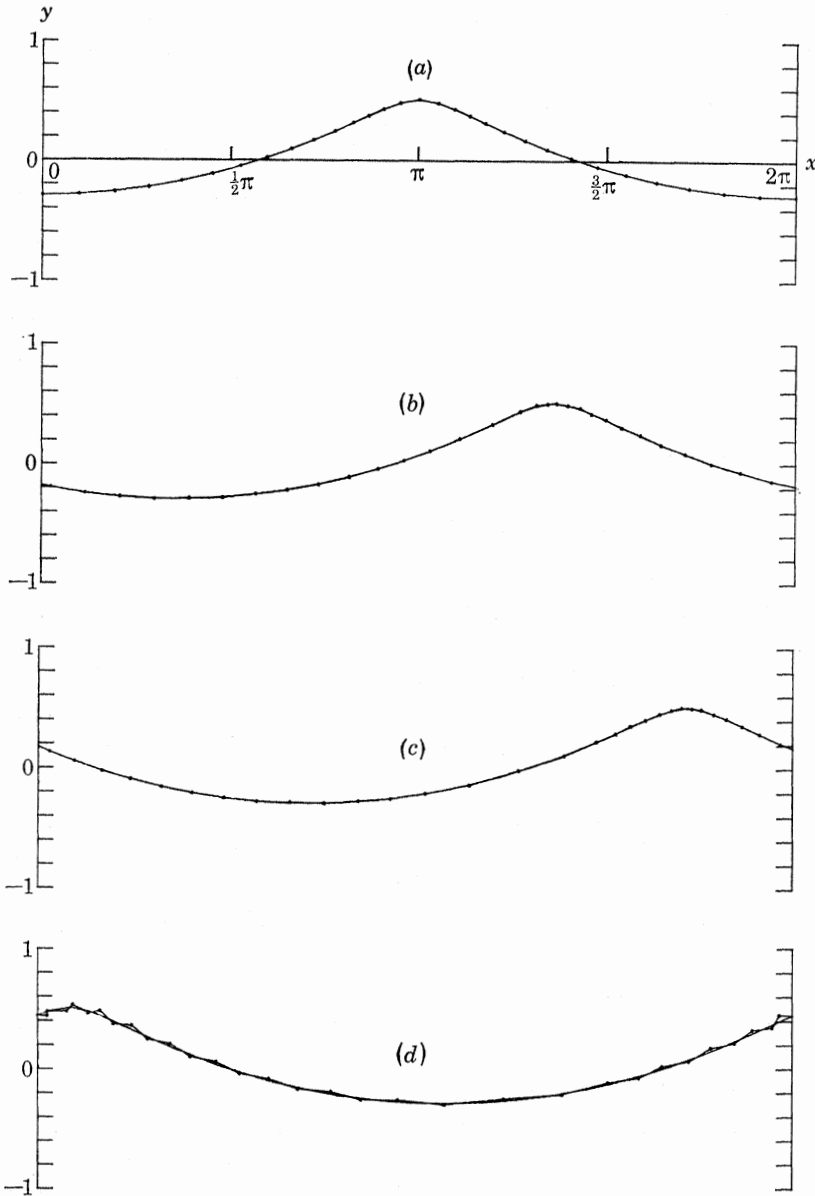


FIGURE 4. Comparison of the profile of a steady progressive wave in deep water ($\delta = 0.80$) computed by Padé approximants from Stokes's series (smooth curve) and the corresponding time-stepped profile (unsmoothed) represented by the circles. $N = 30$. The profiles are compared at times (a) $t = 0$, (b) $t = \frac{1}{3}\pi$, (c) $t = \frac{2}{3}\pi$, (d) $t = \pi$. Note the growth of the instability at $t = \pi$.

Both formulae were tried for smoothing the functions r_j , θ_j and ϕ_j , at every 5, 10 or 20 time-steps. Both worked well and gave a smooth profile with no appearance of the small-scale oscillations. For certain reasons, as stated in the following section, the formula (8.3) was generally preferred.

9. TEST ON A PROGRESSIVE WAVE

An important and essential test of the method was as follows. For initial conditions we took a symmetric, progressive wave of finite amplitude in deep water (see figure 4). A very accurate method of computing the wave profile, based on Stokes's expansion (1880*b*) has recently been developed by Schwartz (1972, 1974). This uses Padé approximants to sum otherwise divergent series. In fact we adopted a modification of Schwartz's method due to Cokelet (1975) in which the expansion parameter is taken as

$$\delta = 1 - q_{\text{crest}}^2 q_{\text{trough}}^2 / c^4, \quad (9.1)$$

where q_{crest} and q_{trough} denote the particle velocities at the wave crest and the wave trough, in a frame of reference moving with the phase-speed c .

We selected a wave corresponding to $\delta = 0.80$, whose crest-to-trough height is about 90% of that of the highest wave in deep water. As initial values for the numerical integration, we inserted the computer coordinates of the wave profile (see figure 4) and the corresponding values of the velocity potential ϕ , *in the frame of reference for which the deep water was at rest*, and therefore the motion generally is time-dependent.

In figure 4 the initial wave has its crest at $x = \pi$, and the wave progresses from left to right. At time intervals of $\frac{1}{3}\pi$, two wave profiles are plotted: the continuous curve represents the Padé-approximated profile, and the plotted points represent the positions of surface particles found from numerical time-stepping by the present method (with $N = 30$).

The plotted points in figure 4 are without smoothing, and the growth of the saw-toothed instability from the third to the fourth profile is apparent. Actually, the unstable wave is found to conserve total energy to one part in 100 up to $t = \pi$, when the computations break down.

Figure 5 now shows the computed points, compared with the steady-wave profile, at time $t = 2\pi$, when smoothing has been applied after every 5 time-steps. As can be seen, the profiles are indistinguishable except to the sharpest eye. For this particular plot the 7-point smoothing formula (8.4) was used. The flux Ω of equation (7.1) varied between 5×10^{-6} and 4×10^{-3} , hovering around 10^{-4} for most of the calculation and showing no tendency to increase. The mean surface displacement \bar{y}_s varied from 3×10^{-5} to 1×10^{-3} . The total energy E lay between 0.06938 and 0.07007 (the value from Padé-approximants is 0.06995). The wave energy decreased by 0.14% at each smoothing with the 7-point formula, compared with 0.06% using the 5-point formula. Although asymptotically less accurate, the 5-point formula

seemed to perform better in practice. When the number N of integration points was raised to 60, only 0.003 % of the energy was then lost at each smoothing.

The numerically calculated profile also remained very closely in-phase with the Padé-approximated profile, using the calculated phase speed of the steady wave.

These checks suggest strongly that the numerical method remains accurate over the time-scales in which we are interested, which are of the order of one wave period.

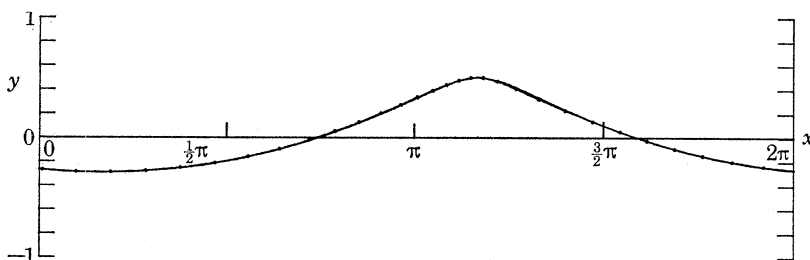


FIGURE 5. Comparison of the profile of a steady wave calculated from Stokes's series (smooth curve) and the corresponding time-stepped profile, with smoothing, represented by circles, at time $t = 2\pi$. (This is twice the maximum duration in figure 4.) $N = 30$; 7-point smoothing every 5 time-steps. The two profiles are indistinguishable.

10. PLUNGING BREAKERS

So far we have described a numerical method of calculating the form of periodic gravity waves in deep water, when these are subjected to an arbitrary application of pressure p_s at the surface; and we have shown that in the special case of free, progressive waves ($p_s = 0$) the method gives results in very close agreement with known theory. In this section we shall show that the method can also yield an accurate description of highly nonlinear and unsteady waves.

There is one feature of the fluid motion which is beneficial to our numerical solutions. As mentioned in §8 in connection with the instability, the straining motion in the primary wave results in horizontal convergence near the wave crest. Two adjacent fluid particles will move closer together as they pass up the forward face towards the crest of the wave. This causes a bunching of the marked particles used in the computation, which has the desirable effect of improving the resolution near a region of sharp curvature. This will be evident in some of the profiles to be shown.

Unlike the situation for steady, symmetric waves, in which the flows are described by a restricted range of parameters corresponding to wave height, wavelength and mean depth, unsteady waves have a much larger diversity, corresponding to various initial wave profiles and particle velocities, and to various distributions of applied pressure at the surface.

We present here the results for waves developing from one initial condition and with one particular form of pressure forcing. As initial conditions we take the

symmetric progressive wave of § 9, for which $\delta = 0.80$. The energy E_0 of this wave is 94% of the maximum possible energy E_m of a progressive wave of the same length in deep water (which corresponds to $\delta = 0.92$; see Longuet-Higgins 1975*a*; Cokelet 1975). At time $t = 0$, a wave crest is at $x = \pi$, and the wave progresses from left to right (see figure 6). The pressure applied at the surface is taken to be

$$p_s = \begin{cases} p_0 \sin t \sin(x-ct) & (0 \leq t \leq \pi), \\ 0 & (t \geq \pi). \end{cases} \quad (10.1)$$

Thus p_s consists of a simple sine-wave progressing with the phase-speed c , in quadrature with the surface elevation. The amplitude of p_s increases from zero when $t = 0$ to p_0 at $t = \frac{1}{2}\pi$, and then falls to zero when $t = \pi$, remaining zero thereafter. The forcing is thus limited to one-half of a wave period, after which the wave runs free.

We show the results for four different pressure amplitudes: $p_0 = 0.0729, 0.100, 0.126$ and 0.146 . To resolve the flow near the crest, the number of points N was

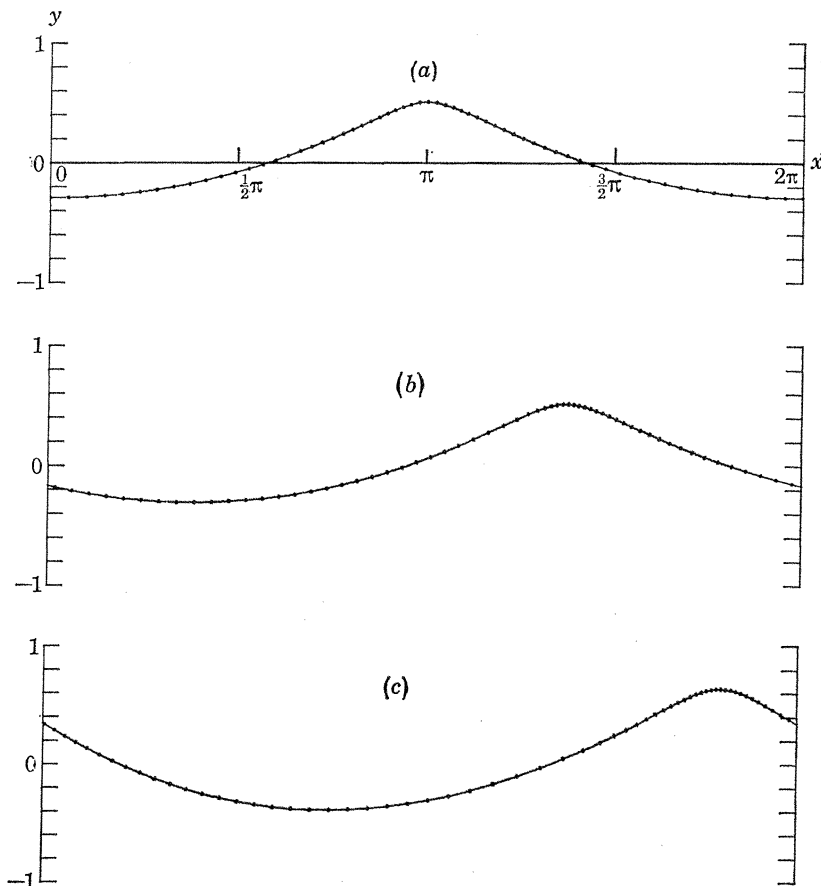


FIGURE 6*a-c*. For description see opposite.

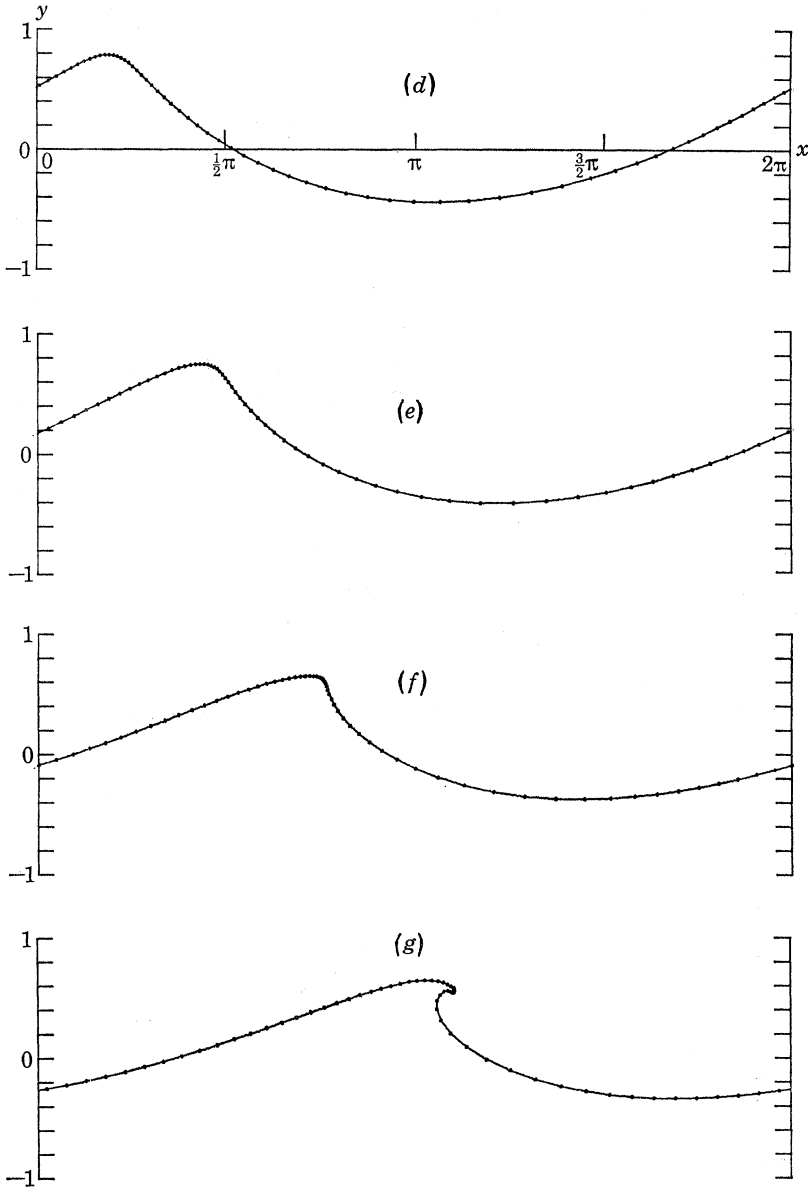


FIGURE 6. A time-sequence of profiles for the pressure amplitude $p_0 = 0.146$ at times (a) $t = 0$, (b) $t = \frac{1}{3}\pi$, (c) $t = \frac{2}{3}\pi$, (d) $t = \pi$, (e) $t = \frac{5}{3}\pi$, (f) $t = \frac{7}{3}\pi$, (g) $t = \frac{8}{3}\pi$. $N = 60$; 5-point smoothing every 5 time-steps. The surface pressure p_0 is applied till $t = \pi$; then the wave runs free.

increased to 60, since 30 points proved too few. The 5-point smoothing formula was used every 5 time-steps.

Figure 6 shows a sequence of wave profiles at various times for $p_0 = 0.146$. The dimensionless time interval between plots is $\frac{1}{3}\pi$, except for the last three plots, which are separated by a time interval of $\frac{1}{3}\pi$. The wave begins at (a) ($t = 0$) as a

steady wave and slowly increases in amplitude as it moves to the right. The pressure forcing is removed at (d) and the wave is thenceforth free. The front face quickly steepens, and at (g) the crest is overhanging.

Figure 7 is a comparison of the profiles of the waves corresponding to $p_0 = 0.0729, 0.100, 0.126, 0.146$ at the same time $t = 5.066$ after applying the pressure. It is clear

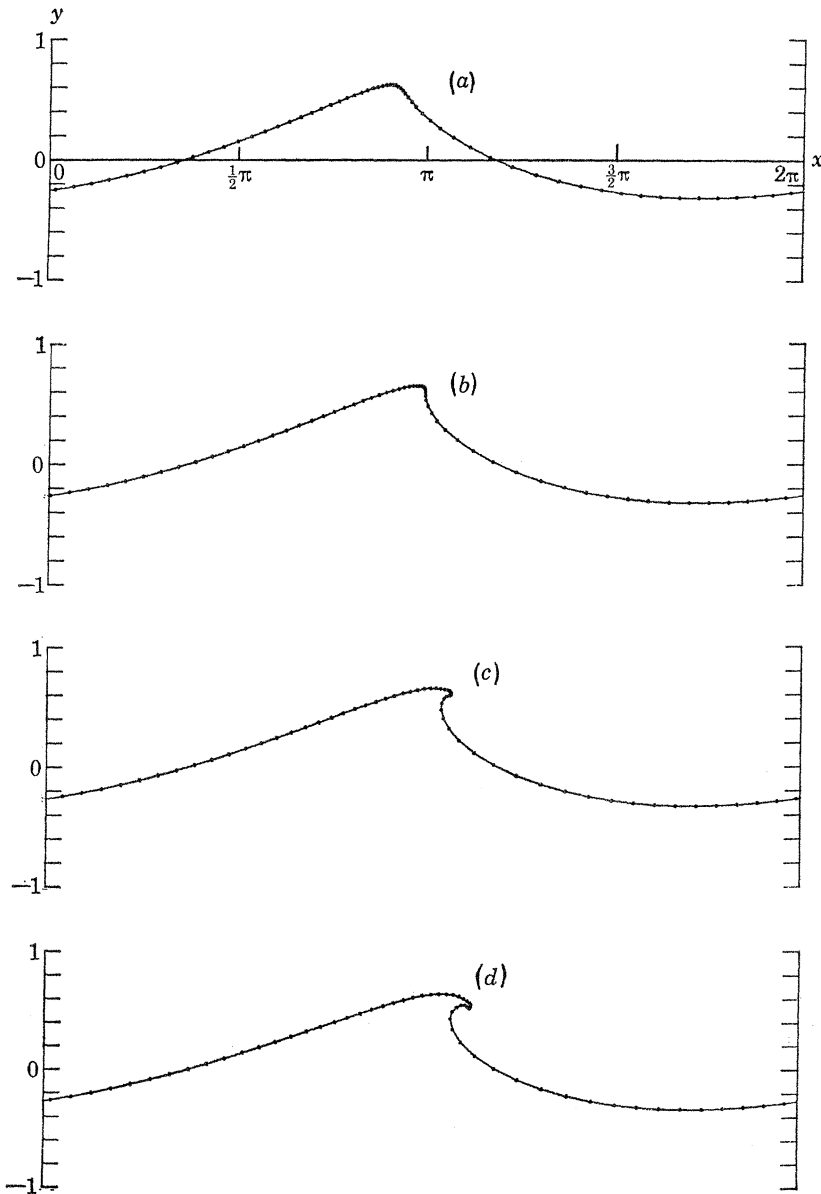


FIGURE 7. A comparison of wave profiles at the same time $t = 5.066$ after first applying the surface pressure. (a) $p_0 = 0.0729$, (b) $p_0 = 0.100$, (c) $p_0 = 0.126$, (d) $p_0 = 0.146$.

that the larger the pressure forcing, the farther towards breaking are the waves. Notice that the profiles remain smooth and free from instability.

Figure 8 shows a close-up of the overturning crests, in the case $p_0 = 0.0729$. This is a series of plots of a small region near the crest of the wave, as seen by an observer moving horizontally with the speed of an infinitesimal wave of the same wavelength (i.e. $(x-t)$ is plotted). The positions of the particles have been marked with small circles, and each profile drawn by connecting adjacent particles with straight lines.

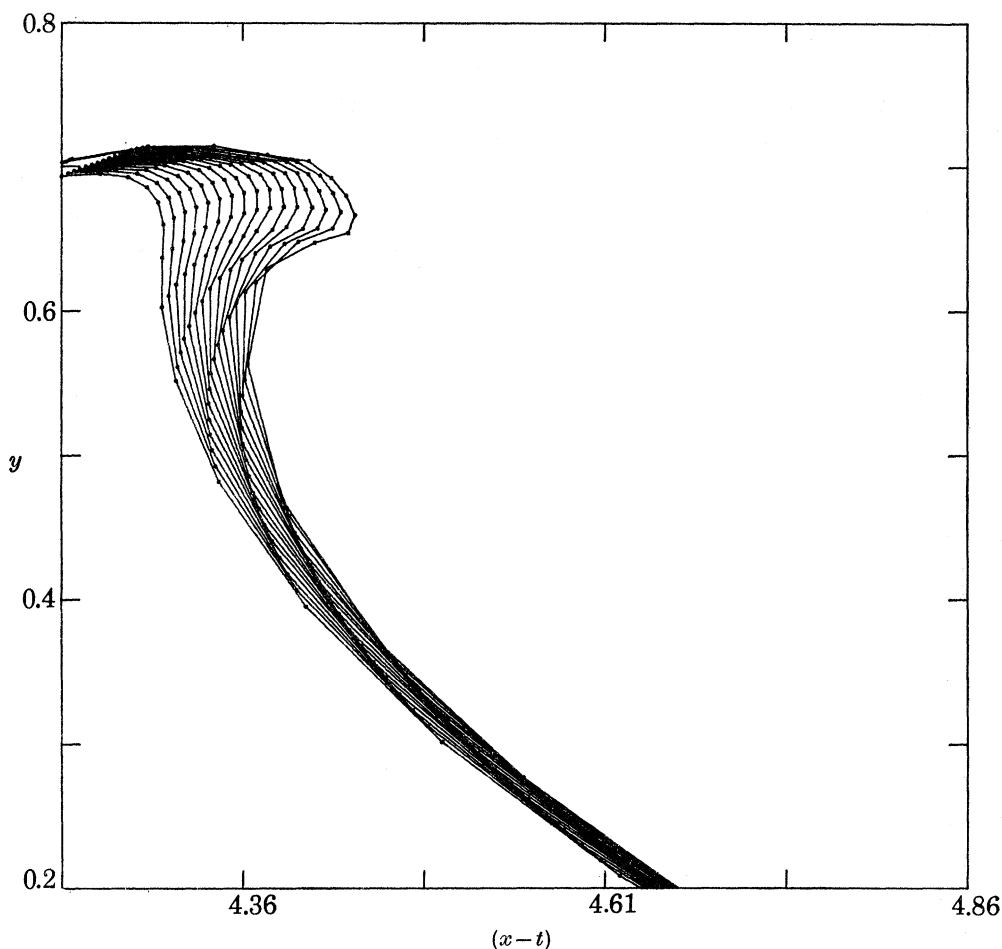


FIGURE 8. Close-up of the wave-crest at successive times, with a plotting interval of $\pi/160$.
 $p_0 = 0.0729$; $5.596 \leq t \leq 5.890$.

On the other hand the imaginary lines joining consecutive positions of each small particle give an idea of the particle trajectories, in this frame of reference.

Similar profiles for the cases $p_0 = 0.100$, 0.126 and 0.146 are shown in figures 9–11.

Perhaps the most remarkable feature of figures 8–11 is that the crest does not tend to develop a sharp angle, as for the highest steady wave, before overturning

takes place. Instead, a smooth jet of fluid is ejected from the forward face of the wave.

Our method of computation appears valid till well after the surface is vertical. However, the curvature at the forward tip of the wave appears to increase in time, so that the computations cannot be continued beyond a certain point.

Figure 12 shows the complete wave profile corresponding to the last wave crest plotted in figures 8–11. We notice a tendency for the more highly forced waves (12 *c*) and (12 *d*), which are also more energetic, to start breaking at lower values of the wave height.

Finally in figures 13–15 we show the time-variation of the kinetic, potential and total energies, respectively, for each value of the forcing pressure p_0 . The oscillations between kinetic and potential energy suggest that there are standing-wave components in the motion. The total energy, however, increases smoothly to a constant value. Also indicated in figure 15 are the values of the final energy E divided by the

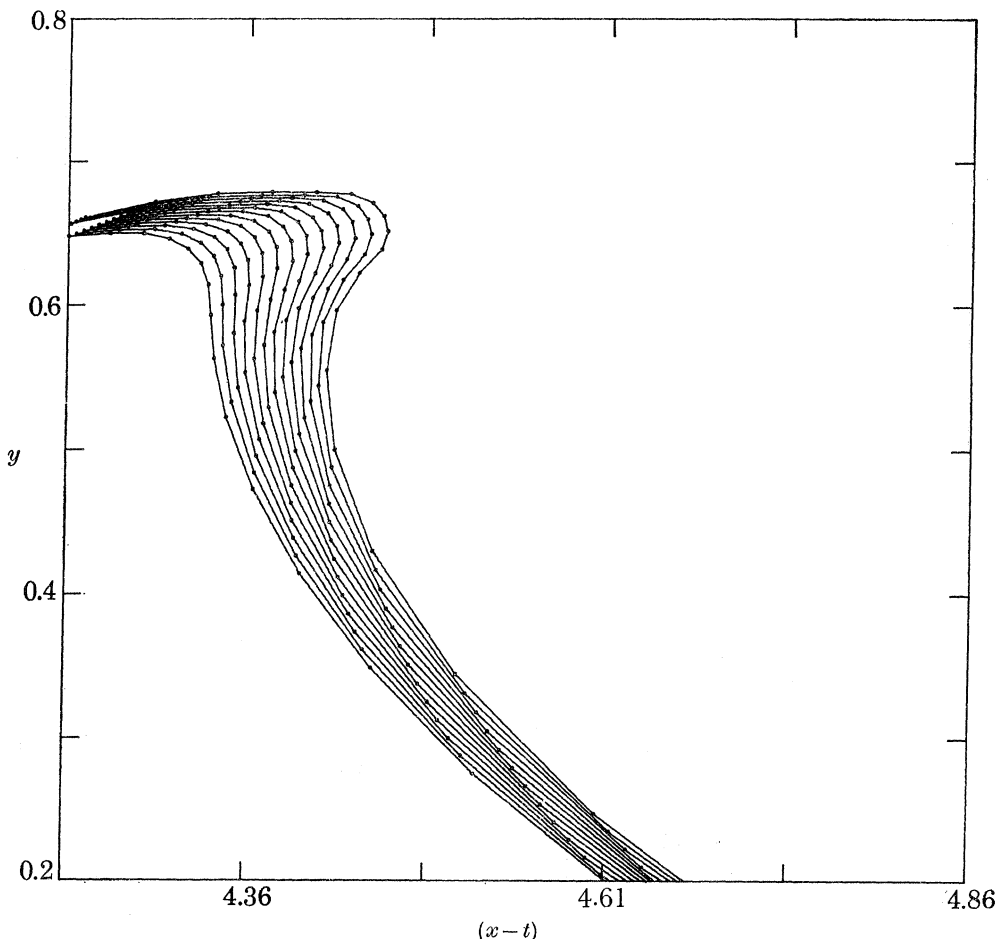


FIGURE 9. As figure 8, but with $p_0 = 0.100$; $5.046 \leq t \leq 5.282$.

energy, E_m , of the most energetic progressive wave, that is $E_m = 0.07403$, for $\delta = 0.92$.

We mention the results of the checks listed in § 7. The flux Ω remained at about 10^{-5} to 10^{-4} for most of the calculation, increasing to 10^{-3} near the end. The mean level \bar{y}_s was of order 10^{-4} for all the calculations, except near the last profile for $p_0 = 0.146$, when it reached 1×10^{-3} . The total energy E remained very constant after $t = \pi$ for all runs, its largest fluctuation being a decrease of about 0.2%.

The above calculations were programmed in FORTRAN IV double precision, and carried out on the I.B.M. 370/165 at Cambridge. The computer time needed for each pressure forcing to achieve overhanging waves was typically 35 min for 270 time-steps at 169 K bytes of storage.

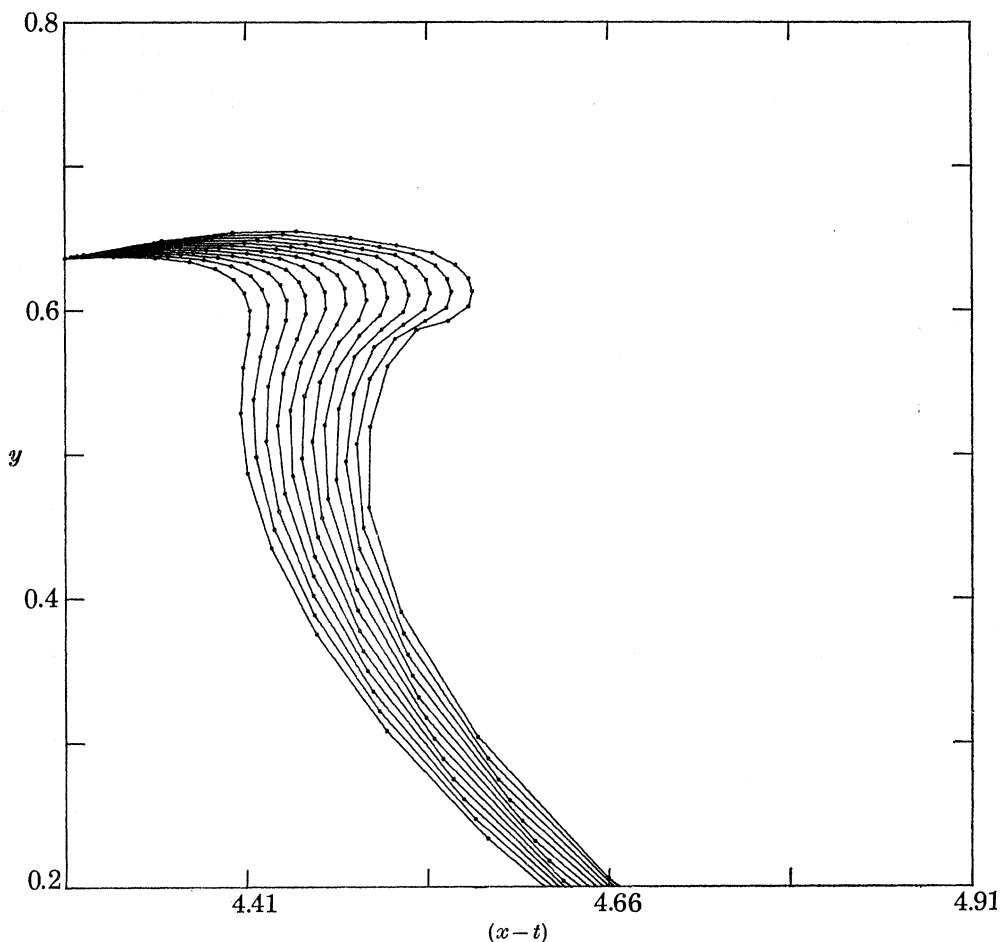


FIGURE 10. As figure 8, but with $p_0 = 0.126$. $4.830 \leq t \leq 5.046$.

11. DISCUSSION AND CONCLUSIONS

We have developed a numerical technique to study nonlinear, unsteady, free-surface waves. Basically the method involves solving an integral equation along the fluid surface to determine the spatial dependence of the motion at each time step. This has the advantage that the only variables which need be calculated and stored are those at the free surface, which is precisely where the flow information is most needed. The surface is represented by marked Lagrangian fluid particles, but our solution technique is neither exclusively Lagrangian nor Eulerian. It makes use of the powerful properties of potential theory by adopting an Eulerian form at each instant of time, and it also makes use of the marked-particle quality of the Lagrangian description by following the fluid particles and their Eulerian velocity potential through time.

It is now possible to follow the development of the surface numerically beyond the

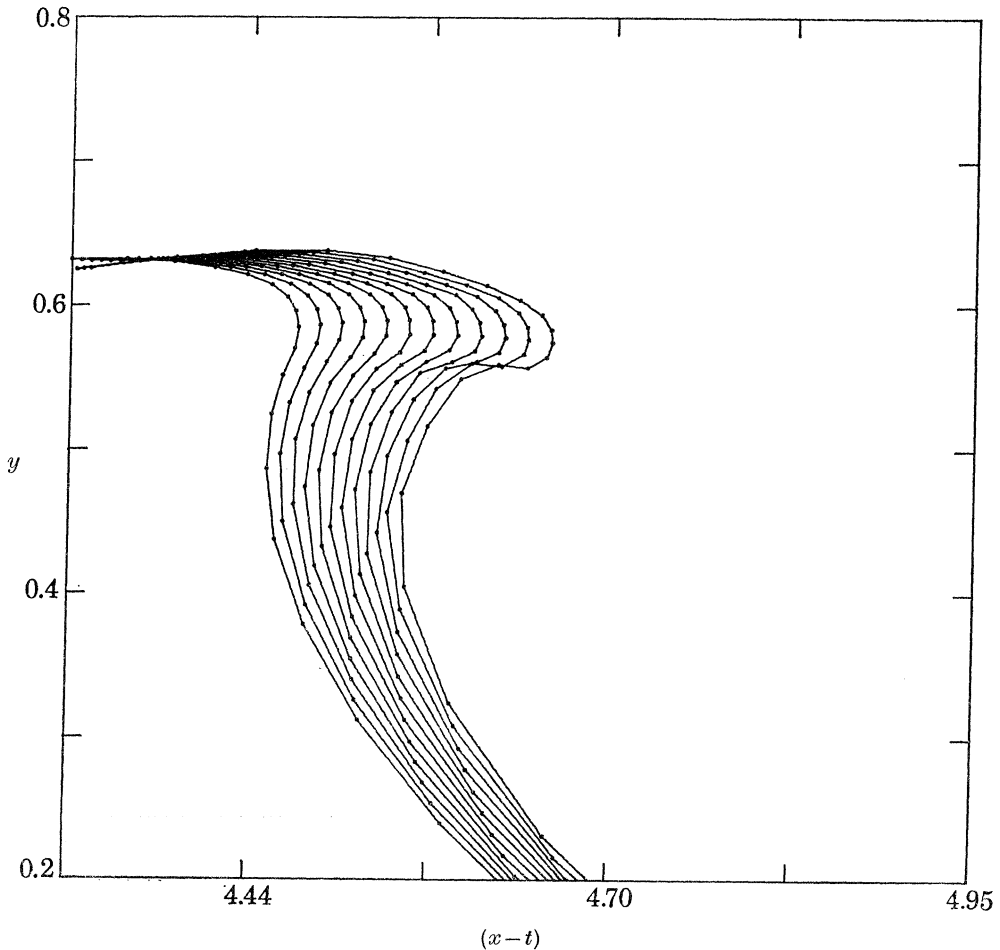


FIGURE 11. As figure 8, but with $p_0 = 0.146$. $4.712 \leq t \leq 4.928$.

instant when the tangent first becomes vertical. From the results of § 10 we conclude that waves do not necessarily develop a sharp corner or singularity before the free surface overturns. Instead they can curl over and plunge towards the forward face of the wave, and there is nothing to suggest that the flow does not remain smooth (neglecting surface tension) up to the instant of impact. The Stokes 120° angle may

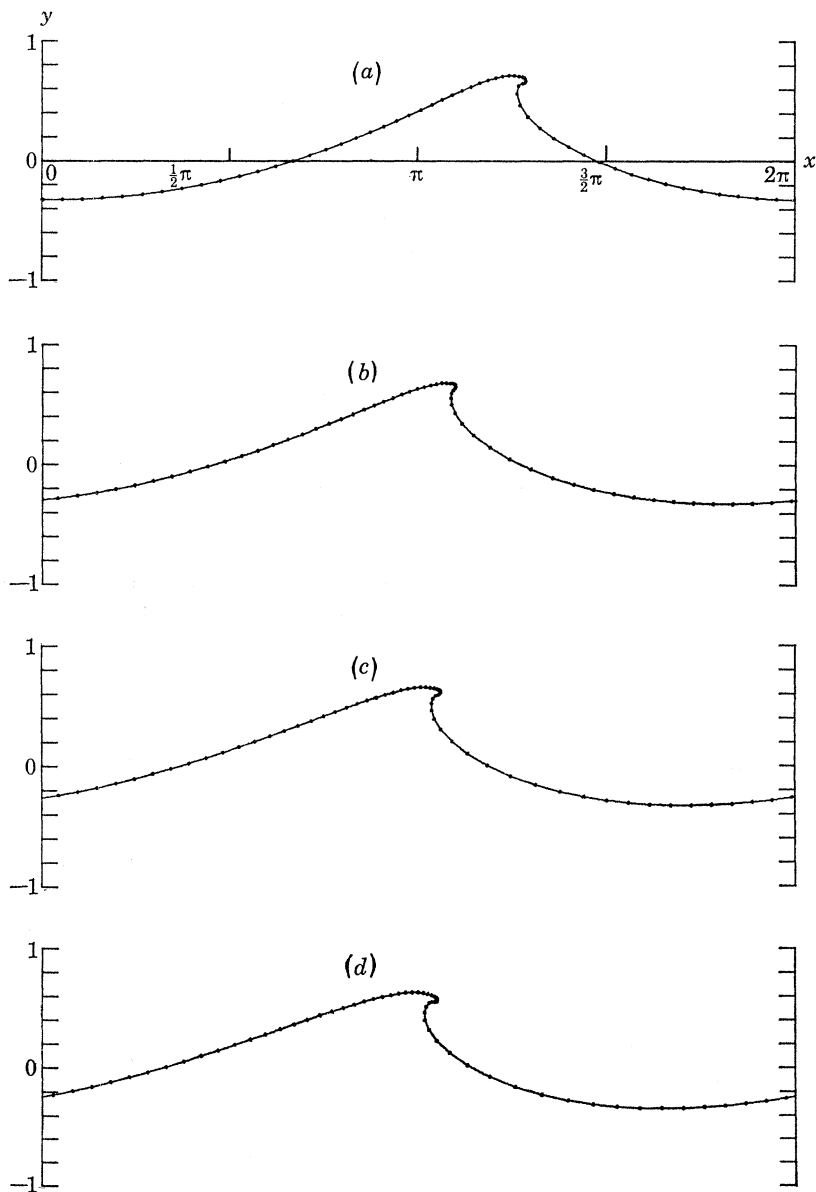


FIGURE 12. A comparison of overturned profiles, for different amplitudes of forcing.
 (a) $p_0 = 0.0729$, $t = 5.890$; (b) $p_0 = 0.100$, $t = 5.282$; (c) $p_0 = 0.126$, $t = 5.046$;
 (d) $p_0 = 0.146$, $t = 4.928$.

not be a typical fluid flow but simply a highly singular form, intermediate between a steady, symmetric wave and an unsteady, unsymmetric, plunging wave. In the gravity-free flows investigated by Longuet-Higgins (1972, 1975*b*) a mass of fluid is deformed into a continually elongated jet with a thin tip. A plunging breaker which is nearly free-falling may behave similarly. It is also possible that most spilling

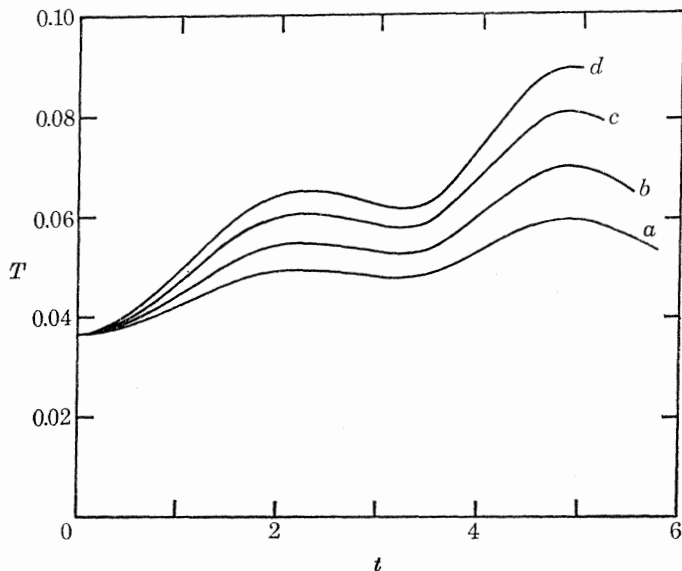


FIGURE 13. The kinetic energy T as a function of the time t , for each pressure amplitude. (a) $p_0 = 0.0729$, (b) $p_0 = 0.100$, (c) $p_0 = 0.126$, (d) $p_0 = 0.146$.

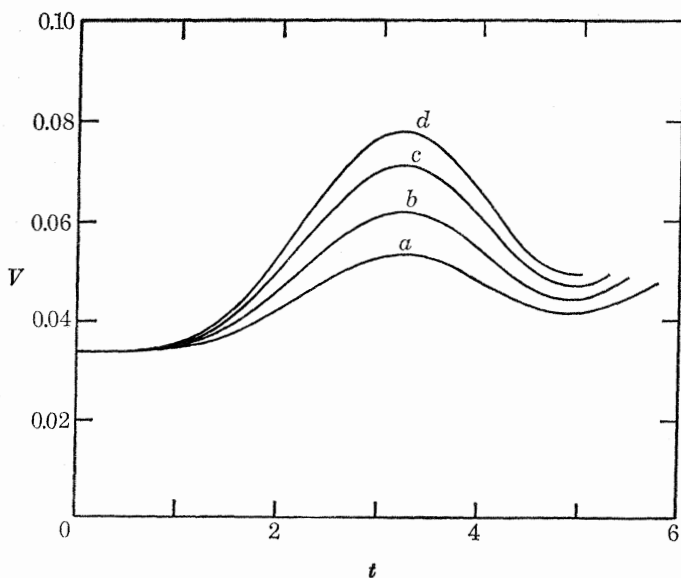


FIGURE 14. The potential energy V as a function of the time t , for each pressure amplitude. (a) $p_0 = 0.0729$, (b) $p_0 = 0.100$, (c) $p_0 = 0.126$, (d) $p_0 = 0.146$.

breakers begin by being similar in form to a plunging breaker, but on a smaller scale, close to the crest of the wave.

In practice, surface tension, air currents and the growth of instabilities may cause the plunging jet to break up into droplets or spray before the tip hits the front face of the wave. In this first study we have neglected surface tension, in order to concentrate on the simpler, large-scale features of the flow.

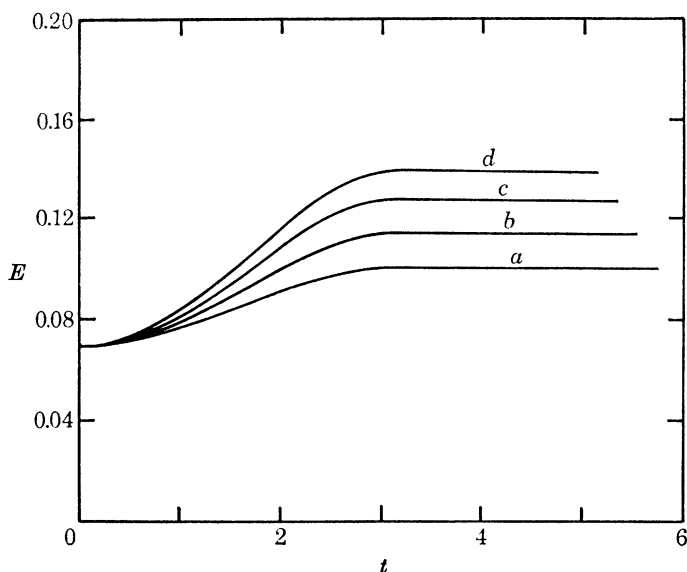


FIGURE 15. The total mean energy ($E = T + V$) as a function of the time t , for each pressure amplitude. (a) $p_0 = 0.0729$, $E/E_m = 1.37$; (b) $p_0 = 0.100$, $E/E_m = 1.55$; (c) $p_0 = 0.126$, $E/E_m = 1.73$; (d) $p_0 = 0.146$, $E/E_m = 1.88$

Our computations, which are for deep water, show incidentally that for the breaking of irrotational waves a sloping bottom is not necessary. Indeed, by eliminating the bottom, one of the parameters of the problem, namely the ratio of the depth to the wavelength, has been eliminated. On the other hand, similar computations can easily be done for periodic waves in water of any arbitrary uniform depth.

By varying the magnitude and duration of the applied surface pressure, it should in future be possible to gain insight into the energy and momentum lost by sea waves by wave breaking, both in deep and shallow water, as a function of the energy input, and hence to gauge the transfer of momentum from the waves to surface currents.

For simplicity we have assumed that the waves are initially progressive. Here again this assumption can be generalized and we can apply the method either to standing waves, or to waves that are a mixture of opposite but unequal progressive waves. These and other possible applications will be studied in future papers.

This computation was begun in March 1972 by one of us (M.S.L.-H.) on the I.B.M. 360/50 at the Institute of Theoretical Astronomy, Cambridge. For the first

two years of his research, E. D. C. was supported by a Graduate Fellowship from the U.S. National Science Foundation, and for a third year by a Research Studentship from the Cambridge Philosophical Society. During a final year, research fees were remitted by Cambridge University. To all these bodies past and present we express our thanks and appreciation.

REFERENCES

- Acton, F. S. 1970 *Numerical methods that work*. New York: Harper & Row.
- Ahlberg, J. H., Nilson, E. N. & Walsh, J. L. 1967 *The theory of splines and their application*. New York: Academic Press.
- Biesel, F. 1952 Study of wave propagation in water of gradually varying depth. In *Gravity waves*. *Circ. U.S. natn. Bur. Stand.* no. 521, pp. 243–253.
- Buckingham, R. A. 1962 *Numerical methods*. London: Pitman.
- Chan, R. K. & Street, R. L. 1970 SUMMAC – A numerical model for water waves. *Tech. Rep. Dep. Civil Engrg, Stanford University, Calif.*, no. 135.
- Cokelet, E. D. 1975 Steady and unsteady nonlinear water waves. Ph.D. dissertation, Cambridge University.
- Gerald, C. F. 1970 *Applied numerical analysis*. Reading, Mass.: Addison-Wesley.
- Longuet-Higgins, M. S. 1953*a* On the decrease of velocity with depth in an irrotational water wave. *Proc. Camb. Phil. Soc.* **49**, 552–560.
- Longuet-Higgins, M. S. 1953*b* Mass transport in water waves. *Phil. Trans. R. Soc. Lond.* **A 245**, 535–581.
- Longuet-Higgins, M. S. 1960 Mass-transport in the boundary layer at a free oscillating surface. *J. Fluid Mech.* **8**, 293–306.
- Longuet-Higgins, M. S. 1972 A class of exact, time-dependent, free-surface flows. *J. Fluid Mech.* **55**, 529–543.
- Longuet-Higgins, M. S. 1975*a* Integral properties of periodic gravity waves of finite amplitude. *Proc. R. Soc. Lond.* **A 342**, 157–174.
- Longuet-Higgins, M. S. 1975*b* Self-similar, time-dependent flows with a free surface. *J. Fluid Mech.* **73**, 603–620.
- Longuet-Higgins, M. S. & Stewart, R. W. 1960 Changes in the form of short gravity waves on long waves and tidal currents. *J. Fluid Mech.* **8**, 565–583.
- Phillips, O. M. & Banner, M. L. 1974 Wave breaking in the presence of wind drift and swell. *J. Fluid Mech.* **66**, 625–640.
- Price, R. K. 1971 The breaking of water waves. *J. geophys. Res.* **76**, 1576–1581.
- Schwartz, L. W. 1972 Analytic continuation of Stokes' expansion for gravity waves. Ph.D. dissertation, Stanford University.
- Schwartz, L. W. 1974 Computer extension and analytic continuation of Stokes' expansion for gravity waves. *J. Fluid Mech.* **62**, 553–578.
- Stokes, G. G. 1880*a* Considerations relative to the greatest height of oscillatory waves which can be propagated without change of form. *Mathematical and physical papers*, vol. 1, pp. 225–228. Cambridge University Press.
- Stokes, G. G. 1880*b* Supplement to a paper on the theory of oscillatory waves. *Mathematical and physical papers*, vol. 1, pp. 314–326. Cambridge University Press.